DESIGN AND EVALUATION OF A THREE-PHASE SOLAR PV AND BATTERY ENERGY STORAGE SYSTEM WITH INTEGRATED UPQC

V.Sai Lokesh, UG Students, Sree Vahini Institute of Science and Technology (Autonomous), Tiruvuru, A.P
K. Syam Kumar, UG Students, Sree Vahini Institute of Science and Technology (Autonomous), Tiruvuru, A.P
P. Srinu, UG Students, Sree Vahini Institute of Science and Technology (Autonomous), Tiruvuru, A.P
T. Shiva Kumar, UG Students, Sree Vahini Institute of Science and Technology (Autonomous), Tiruvuru, A.P
Mrs. Hari Priya, Assist. Professor, Dept of EEE, Sree Vahini Institute of Science and Technology (Autonomous), Tiruvuru, A.P
Dr. K. Kiran Kumar, Assoc. Professor, Dept of EEE, Sree Vahini Institute of Science and Technology (Autonomous), Tiruvuru, A.P

ABSTRACT:
This study investigates the application of Unified Power Quality Conditioners (UPQC) to address grid power quality issues including harmonics caused by non-linear loads. In this study, the Photovoltaic (PV) and Battery Energy Storage System (BESS) assist the UPQC. In most cases, the PV system provides the load with active electricity. However, in the event that the PV fails to generate power, the BESS swings in and supplies electricity, particularly during more durable voltage disruptions. The high degree of environmental dependence and instability of the standalone PV-UPQC system make it less dependable than the hybrid PV-BESS system. As a result, BESS will continually increase the voltage support capability over time, simplify the DC-link voltage management algorithm, and continue to generate clean energy. A self-tuning filter (STF) combined with the unit vector generator (UVG) technology controls the UPQC controller phase synchronization function. By using STF, the UPQC will be able to function effectively in situations when the grid voltage is distorted and imbalanced. Therefore, the STF-UVG is used to generate the synchronization phases for the series and shunt active power filter (APF) compensator in the UPQC controller, eliminating the need for a phase-locked loop (PLL). To demonstrate the importance of the proposed approach, the proposed STF UVG method is lastly contrasted with the conventional synchronous references frame (SRF-PLL) method based UPQC. To further validate the study using MATLAB-Simulink software, a number of case studies are taken into consideration.
Index terms: Unified Power Quality Conditioner (UPQC), Solar Photovoltaic (PV), Self-Tuning Filter (STF), Battery Energy Storage System (BESS) and Power Quality.

INTRODUCTION:

The main ingredient of life is energy. Among the several types of energy, electricity is one of the most important. It guarantees the process of adaptability, and the need for this energy is growing quickly. Over the last few decades, researchers have responded significantly to the phrase "Power Quality," particularly in the field of electrical engineering. Energy efficiency is preserved by covering up for power quality issues, which guarantees stable electrical energy output and promotes grid decarbonisation. When sensitive loads or other equipment trip due to voltage disturbances like harmonics, swells, or sags, industrial plants may suffer negative outcomes, such as the cessation of a process. The industry is accustomed to these situations, which result in significant financial losses. Industrial clients deploy mitigation devices of the series APFs to circumvent this circumstance and protect their plants from grid interruptions [1]– [8]. Modern plants are using more and more power electronics components, which leads to the creation of harmonics and sensitive loads in the system. To address these problems, shunt APFs are used [9]–[12]. As a result, a new trend is created that serves two functions: first, it benefits the utility, and then it benefits the consumers. This trend is significant because it aims to safeguard both the utility and the consumers at the same time, protecting the sensitive components from voltage disruptions and reducing the distortion that the customers' loads cause to enter the utility [13]. In order to control the load voltage and grid current simultaneously, the UPQC model is constructed using a back-to-back arrangement of series and shunt APF compensators [14]. Researchers' interest in working on UPQC has increased due to the present trend of microgrids and distributed generation [15]–[17]. The use of renewable energy sources and a decreased reliance on the finite supply of fossil fuels, which also contributed to global warming, have also drawn more attention. Renewable energy solutions, which also improve power quality and have the flexibility to function when the grid is unavailable, are clearly needed.

In order to successfully minimize PQ concerns on the grid side by offering genuine power supply during voltage interruption, a fuel cell (FC) linked with UPQC is suggested in [19]. However, neither the decarbonisation of the grid-connected system nor the integration of renewable energy supplies with UPQC were emphasized in their study. A PV integrated with UPQC is suggested in [20], [21] to provide sustainable energy and address power quality issues. However, their investigation did not take into account profound voltage sag or prolonged interruption. Additionally, the problem of prolonged interruption is resolved by the dynamic voltage restorer (DVR) coupled with the superconducting magnetic energy storage system (SMES) to sustain the load for an extended period of time [22]. However, the problem of current related harmonics was not taken into account. Under such circumstances, the PV UPQC can be interfaced with an energy storage system such as BESS, which can be a huge help in continuously supplying the load with actual power. BESS is crucial for renewable energy systems while UPQC is functioning independently.

When the system is used for critical loads like semiconductor companies, hospitals, etc., where a continuous supply of the highest quality power is crucial, the additional expense of the BESS is justified. Consequently, the PV supports the UPQC and the BESS was designed in this effort. A DC-DC buck-boost converter connects the BESS to the DC-link, and a DC-DC boost converter connects the PV to the DC-link [23], [24]. In order to improve the reliability of the distribution power system, the BESS activates and delivers power when the PV system is unable to supply it, particularly during longer-term voltage interruptions. Normally, the PV system provides the active power to the load. Researchers attempt to create the DC-link voltage control algorithm in [19] and [25]– [27] in order to guarantee a steady and consistent DC-link capacitor voltage. However, the UPQC controller computational load and complexity increased. But since PV-BESS can sustain a UPQC DC-link capacitor externally and lessen the strain on the DC-link capacitor, it could be a preferable option.

The synchronization phase is one of the most important aspects of UPQC system control. For the shunt and series APF compensators to generate reference current and voltage, respectively, precise synchronization phase operation is necessary [28]. The UPQC should be able to inject the voltage and current in phase with the grid in order to carry out the synchronization operation efficiently. For the synchronization phase algorithm, the majority of UPQC controllers in [15]– [21] are created using a traditional SRF-PLL, which is unable to handle distorted and imbalanced voltage grid conditions. Additionally, a low pass filter in a traditional PLL controller adds phase delay to the synchronization process, resulting in undesirable reference current and voltage ripples. Additionally, a PLL PI controller adds complexity to the control and necessitates time-consuming fine tweaking [29]. Using the STF, which has superior phase tracking and basic component extraction capabilities, is one potential remedy for the phase detection synchronization. This work uses the construction of unit vectors made up of sine and cosine functions for the extraction of harmonic current algorithms and voltage error algorithms in order to create a basic controller structure based on its operating principle.

Additionally, the unit vector synchronization phases are applied to the reference current generation in shunt compensators that are designed with integration and strength STF using the direct-quadraturezero (STF-dq0) operating idea, which is independent of all PLL components. The reference voltage generation in the series compensator will likewise use the dq0 working idea in conjunction with synchronization phases for in-phase compensation. Above all, the suggested method that will be used with the UPQC controller must be better and more dependable while handling distorted and imbalanced power grid conditions. In order to attain almost unity power factor, it can additionally preserve sinusoidal grid current while controlling the appropriate load voltage and reducing the phase difference.

This research suggests using PV and BESS coupled in tandem with UPQC to address complicated power quality issues, particularly when there is a prolonged voltage interruption. For verification of the dynamic performance of the proposed UPQC coupled with PV and BESS, a variety of case studies are used. The performance of UPQC with a DC-link capacitor alone and UPQC with PV and BESS incorporated is also contrasted. In order to overcome the shortcomings of the traditional PLL, the STF combined with the UVG technology (STF-UVG) is also used to generate the synchronization phases for the UPQC controller. In order to verify the superiority of the suggested method, a performance comparison between the STF-UVG and a conventional SRF-PLL is conducted. The performance of the proposed UPQC system is then examined under dynamic conditions using MATLAB-Simulink software.

SYSTEM DESIGN:

Fig. 1 shows when PV-BESS-UPQC is constructed. The PV-BESS-UPQC model is the basis for the three-phase system design. The PV-BESS-UPQC is made up of a DC-link split capacitor connected to a series and shunt APF compensator. The PV array and batteries are connected to the DC-link in parallel. A boost converter connects the PV to the DC-link. Additionally, a buck-boost converter connects the BESS to the DC-link. The series compensator compensates for supply voltage sags, swells, interruptions and harmonics by acting as a regulated voltage source. Conversely, the shunt compensator reduces the load current harmonics. Interfacing inductors are used to connect the shunt and series APF compensators.

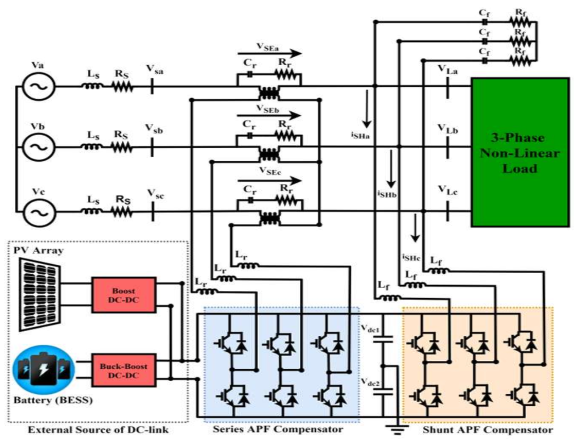

Fig. 1. Configuration of the UPQC system

The converter switching process causes harmonics to be produced, hence a ripple filter is used to remove them. A series injection transformer is used by the series compensator to add voltage to the grid. A three-phase non-linear load is used in this work. The precise measurement of the PV array, split capacitor, DC-link reference voltage, etc., is the first step in the PV-BESS-UPQC design process. The shunt compensator is designed to regulate the PV array peak output power in addition to reducing current harmonics. The PV array is built so that its maximum power point (MPP) voltage is equal to the reference DC-link voltage since it is directly linked to the UPQC DC-link. Under normal conditions, the PV array rating guarantees that it will transmit the load active power as well as electricity to the grid and the BESS for charging. Furthermore, the BESS is built to supply the

ISSN: 2278-4632
Vol-15, Issue-04, No.03, April: 2025

inadequate power equal to the drop in DC-link voltage when the PV array produces less power than the DC-link load requirement. Furthermore, the BESS can satisfy the entire load requirement in the event that the PV array is not producing any electricity.

DESIGN OF UPQC:

MAGNITUDE OF DC-LINK VOLTAGE:

The DC-link voltage, $\boldsymbol{Vdc}$, $\boldsymbol{min}$ minimum values depend on the system phase-voltage. It is required that the DC-link voltage magnitude be almost double the supply peak phase voltage. The formula for $\boldsymbol{Vdc}$, $\boldsymbol{min}$ is as follows:

$$\mathbf{V_{dc,min}} = \frac{\mathbf{2\sqrt{2}(V_{LL,rms})}}{\mathbf{\sqrt{3}m}} \quad \dots \quad (1)$$

where $\boldsymbol{m}$ denotes the modulation depth index, which is allocated to 1 and $\boldsymbol{VLL}$, $\boldsymbol{rms}$ denotes the grid phase-voltage, which is 400 $\boldsymbol{Vrms}$ as determined by the Malaysian Energy Commission in accordance with IEC standards. Thus, with a $\boldsymbol{VLL}$, $\boldsymbol{rms}$ of 400 $\boldsymbol{Vrms}$, V$\boldsymbol{dc}$,$\boldsymbol{in}$ is determined as 653.2 $\boldsymbol{V}$. After taking into account the value of PV-BESS as the external source of DC-link, the DC-link voltage, V, is determined to be 700 V.

VALUE OF DC-LINK CAPACITOR :

The DC-link capacitor equation is expressed as follows:

$$\mathbf{C_{dc,min}} = \frac{\mathbf{3V_{ph}i_{sh}a_f k_e t}}{\mathbf{1/2\left(V_{dc,set}^2 - V_{dc,min}^2\right)}} \quad \dots \quad (2)$$

In the present situation, Vdc, set indicates the voltage that is equivalent to the reference voltage, Vdc, in indicates the minimum required voltage of the DC-link, Vph indicates the phase-voltage, ish indicates the phase-current for shunt APF, af indicates the overloading factor, t indicates the time to reach the steady-state, and ke indicate the energy variation during dynamic conditions. The observed value of Cdc, min is 9330.28 µF, and it is about 9400µF. The estimated minimum voltage of the DC link, Vdc, min = 677.69 V, Vdc, set = 700 V, Vph = 230.9 V, ish = 57.5 A, t = 30 ms, a = 1.2, and energy fluctuation during dynamics = 10% (ke = 0.1). After that, two split capacitors are each set to 4700µF.

SHUNT APF INDUCTOR RIPPLE FILTER:

The shunt APF is attached through an inductor with the network as a passive filter which relies on the switching frequency denoted as fSH, Icr, pp denotes ripple current and Vdc, set denotes the DC-link voltage. The interfaced inductor equation is shown as follows:

$$\boldsymbol{L_{f,min}} = \frac{\boldsymbol{\sqrt{3}(m)(V_{dc,set})}}{\boldsymbol{12(a_f)(f_{SH})(I_{cr,pp})}} \quad \dots \quad (3)$$

In this case, m denotes the modulation depth, af the maximum overload value in pu units, Icr, pp the inductor ripple current, which is 20% of the shunt APF rms phase current. The frequency of switching is indicated by fSH. With fs = 10 kHz, m = 1, VDC = 700 V, a = 1.5, and Icr, min = 20%, the value of Lf, min is measured as 1.79 mH. In this inquiry, the specified value, which is 3mH, is taken into consideration.

THREE-PHASE ISOLATION TRANSFORMER FOR SERIES INJECTION :

APF series VSC connected to the grid in series. The transformer voltage rating is dependent on both the DC-link voltage and the necessary voltage injection. VSE is determined to be 138.54V, the voltage to be injected, in order to compensate for a voltage variance of ±60%. At 700V DC-link voltage, the series compensator modulation index drops in such scenario. The injection transformer's maximum value turns ratio for the series APF can be written as follows:

ISSN: 2278-4632
Vol-15, Issue-04, No.03, April: 2025

$$K_{SE} = \frac{V_{LL\,rms}}{\sqrt{3}(V_{SE})} \quad \ldots \quad (4)$$

Where the KSE is computed, it is around 1.667 to 2. The injection transformer's VA rating is stated as follows:

$$S_{SE} = 3(V_{SE})\left(i_{SE(under\,sag)}\right) \quad \ldots. \quad (5)$$

The grid current is equal to the current flowing across the series APF. The supply current is 36A when the voltage sag condition is 0.6 pu. As a result, 15 kVA is the injection transformer attained VA rating.

SERIES APF INDUCTOR RIPPLE FILTER :

As a passive filter that depends on the DC-link voltage, ripple current, and switching frequency, the series APF is connected to the network via an inductor. The following is an illustration of the interfaced inductor equation:

$$L_{r,min} = \frac{\sqrt{3}(m)(V_{dc,set})(K_{SE})}{12(a_f)(f_{SE})(I_{cr})} \quad \ldots \quad (6)$$

In this case, m stands for modulation depth, a for maximum overload value per unit and Ir for inductor ripple current, which is calculated as 20% of Series APF rms phase current. The switching frequency is indicated by fSE. With m = 1, Vdc, Vet = 700 V, af = 1.5, fSE = 10 kHz and 20% ripple current, the observed inductor value is 3.6 mH.

DESIGN OF UPQC CONNECTING WITH PV-BESS AS EXTERNAL SUPPORT OF DC-LINK:

The PV system, BESS, boost converter, buck-boost converters and controller comprise form the recommended model shown in Fig. 2. In employing a buck-boost converter to connect the BESS in parallel to the DC-link capacitor, the UPQC stability is enhanced to address the power quality issue. The overall power flow in the model is represented by (7).

$$\mathbf{P_{total} = P_{pv} + P_{BESS} - P_{Load\ DC-link}} \quad \ldots \ (7)$$

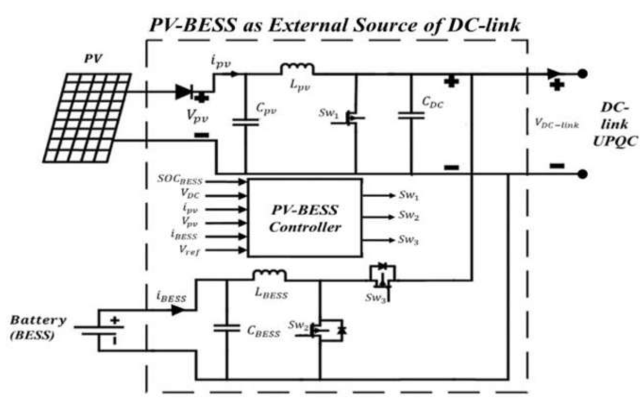

Fig.2. Configuration of the PV-BESS system

MODELLING OF PV SYSTEMS:

The PV model from the Simulink package is used in this study. A number of parallel-connected strings of PV modules make up the PV model. Additionally, each string contains series PV modules that provide the necessary power, voltage and current ratings. As shown in Fig. 3, a single-diode equivalent circuit can be used to resemble each PV cell in a module. A current source linked in parallel with a forward diode, a series-connected resistance and a parallel-connected resistance make up the single-diode equivalent circuit. The PV cell begins to generate electricity as soon as it detects sunshine.

The output current of a PV cell is calculated using Kirchhoff's current law as follows:

$$i_{pv} = i_{ph} - i_d - i_{sh} \quad \ldots \quad (8)$$

The photocurrent is represented by iph in this specific instance, the current flowing across the forward diode by id and the current flowing across the shunt resistance by ish. The following describes methods to replace id and ish in (9) with suitable expressions:

$$i_{pv,c} = i_{ph} - i_s \left[exp^{\left(\frac{Q(V_{pv}+i_{pv,c}R_S)}{\eta K T_c}\right)} - 1 \right] - \frac{V_{pv,c} + i_{pv,c}R_S}{R_{sh}} \quad \ldots \quad (9)$$

where k represents the Boltzmann's constant (1.381 x 10-23 J/K), Tc indicates the actual temperature of the cell (°C), Vpv, c indicates the cell output voltage (V), ipv, c indicates the cell output current (A), η denotes the diode ideality factor following the type of PV cell technology (Si-mono) which is 1.2 used in this work, k denotes the Boltzmann's constant (1.381 x 10-23 J/K), Rsh indicates the shunt resistance of the cell (Ω), and Rs indicates the cell series resistance (Ω).

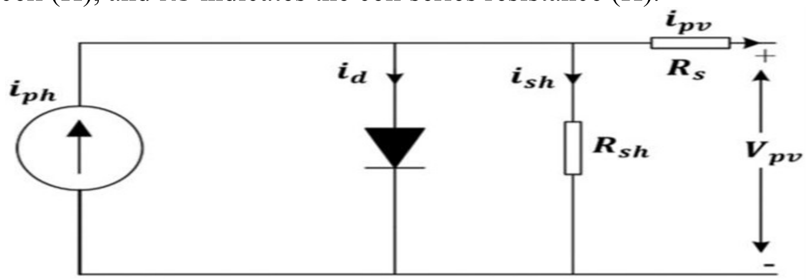

Fig. 3. Single-diode PV cell equivalent circuit

Principle of Operation of the Proposed PV-BESS-UPQC Control Using Self-Tuning Filter Technique

METHOD OF STF-UVG SYNCHRONIZATION:

The proposed STF-UVG methodology is non-iterative and uses an easy strategy to extract the synchronization phases from the supply voltage. The STF approach in the UPQC controller system is seen in Fig. 4. The three-phase supply voltage is shown in matrix form in (10) and the source voltage is changed from the abc-domain to the $\alpha\beta 0$-domain using the Clarke transformation matrix.

$$\begin{bmatrix} V_{s\alpha} \\ V_{s\beta} \\ V_{s0} \end{bmatrix} = \sqrt{\frac{2}{3}} \begin{bmatrix} 1 & -\frac{1}{2} & -\frac{1}{2} \\ 0 & \frac{\sqrt{3}}{2} & -\frac{\sqrt{3}}{2} \\ \frac{1}{2} & \frac{1}{2} & \frac{1}{2} \end{bmatrix} \begin{bmatrix} V_a \\ V_b \\ V_c \end{bmatrix} \quad \ldots \quad (10)$$

In the $\alpha\beta$-domain, the distorted supply voltage is divided into fundamental and harmonic components by taking into account just two phases. This association is seen in (11)

$$\begin{bmatrix} V_{S\alpha} \\ V_{S\beta} \end{bmatrix} = \begin{bmatrix} V_{S\alpha(fund)} + V_{S\alpha(har)} \\ V_{S\beta(fund)} + V_{S\beta(har)} \end{bmatrix} \quad \ldots \quad (11)$$

The harmonic (har) component in the $\alpha\beta$ domain is shown by Vs, (har), whereas the fundamental (fund) component is indicated by Vs, $\alpha(fund)$. Each are essential for the production of synchronization phases in the $\alpha\beta$-domain. Through the use of the self-tuning filtering (STF) technique, the essential elements. To suppress the harmonic components that are present in the distorted supply voltage, the STF approach is used. Consequently, the quality of the extraction is enhanced and the synchronization phases are extracted more precisely.

SERIES APF COMPENSATION CONTROL :

The STF-UVG phase and frequency information is used in (12) to compute the three-phase reference voltage signal, $Vref, abc*$ in the abc domain. At this point the basic load voltage peak amplitude yields the value of the maximum peak voltage magnitude, Vm, $max\text{–}peak$. The reference voltage signal should be in phase with the supply voltage at PCC; the components of the q-frames should be zero, and the peak amplitude load reference voltage is represented by the d-frames.

$$\begin{bmatrix} V_{refa}^{*} \\ V_{refb}^{*} \\ V_{refc}^{*} \end{bmatrix} = V_{m\,\max-peak} \begin{bmatrix} \sin(\omega t) \\ \sin(\omega t - \frac{2\pi}{3}) \\ \sin(\omega t + \frac{2\pi}{3}) \end{bmatrix} \quad \dots \quad (12)$$

$$\begin{bmatrix} V_{ref\alpha}^{*} \\ V_{ref\beta}^{*} \\ V_{ref}^{*} \end{bmatrix} = \sqrt{\frac{2}{3}} \begin{bmatrix} 1 & -\frac{1}{2} & -\frac{1}{2} \\ 0 & \frac{\sqrt{3}}{2} & -\frac{\sqrt{3}}{2} \\ \frac{1}{2} & \frac{1}{2} & \frac{1}{2} \end{bmatrix} \begin{bmatrix} V_{refa}^{*} \\ V_{refb}^{*} \\ V_{refc}^{*} \end{bmatrix} \quad \dots \quad (13)$$

$$\begin{bmatrix} V_{refd}^{*} \\ V_{refq}^{*} \end{bmatrix} = \begin{bmatrix} \cos(\omega t) & \sin(\omega t) \\ -\sin(\omega t) & \cos(\omega t) \end{bmatrix} \begin{bmatrix} V_{ref\alpha}^{*} \\ V_{ref\beta}^{*} \end{bmatrix} \quad \dots \quad (14)$$

The three-phase reference voltage signal is then shown in matrix form in (13) and converted from the abc domain to the $\alpha\beta0$-domain using the Clarke transformation matrix. Next, the proposed STF-UVG is used to create synchronization phases and frequency, which are then utilized to produce the reference axis in the dq-frames. This allows for the extraction of the fundamental component of the distorted supply voltage at PCC. The reference voltage signal is obtained in the dq frames using (14) and the Park transformation matrix, bringing into account just two phases. Additionally, the three-phase load voltage, VL, αbc, is transformed from the abc-domain to the $\alpha\beta0$-domain using the Clarke-matrix and Equation (15). Then, as shown in (16), the load voltage signal in the $\alpha\beta0$-domain is transformed by taking into account just two phases in dq-frames utilizing a Park-matrix with the frequency and synchronization phases from STF-UVG for creating the reference axis in the dq-frames.

$$\begin{bmatrix} V_{L\alpha} \\ V_{L\beta} \\ V_{L0} \end{bmatrix} = \sqrt{\frac{2}{3}} \begin{bmatrix} 1 & -\frac{1}{2} & -\frac{1}{2} \\ 0 & \frac{\sqrt{3}}{2} & -\frac{\sqrt{3}}{2} \\ \frac{1}{2} & \frac{1}{2} & \frac{1}{2} \end{bmatrix} \begin{bmatrix} V_{La} \\ V_{Lb} \\ V_{Lc} \end{bmatrix} \quad \dots \quad (15)$$

$$\begin{bmatrix} \boldsymbol{V_{Ld}} \\ \boldsymbol{V_{Lq}} \end{bmatrix} = \begin{bmatrix} \cos(\omega t) & \sin(\omega t) \\ -\sin(\omega t) & \cos(\omega t) \end{bmatrix} \begin{bmatrix} \boldsymbol{V_{L\alpha}} \\ \boldsymbol{V_{L\beta}} \end{bmatrix} \quad \dots \quad (16)$$

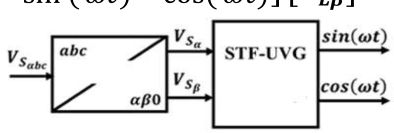

(a)

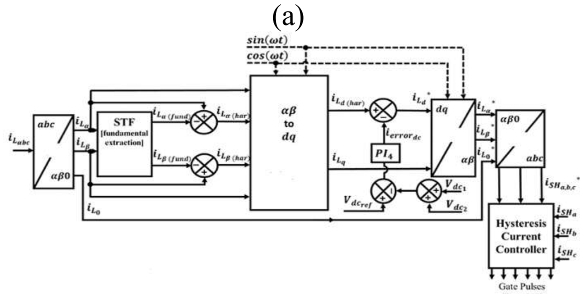

(b)

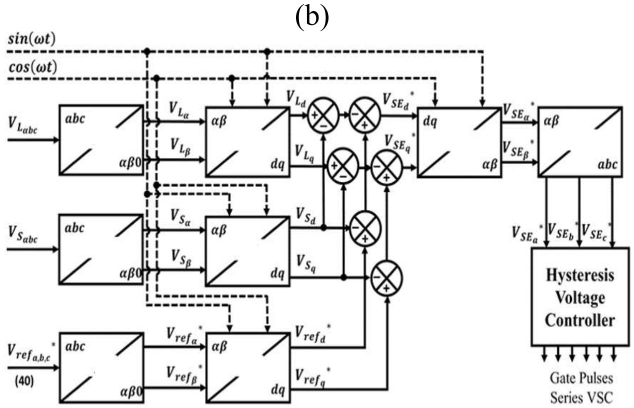

(c)

Fig. 4. Control block diagram for the UPQC controller scheme self-tuning filter (STF) approach STF-UVG (a) Shunt APF (b) Series APF (C) control schemes.

SIMULATION RESULTS :

Performance evaluation, PV-BESS-UPQC control system design, and the connection of the proposed PV BESS-UPQC circuits are all included in the simulation studies. A common DC-link, which consists of the DC link capacitor, PV and BESS, is shared by a conventional two-level inverter for the shunt and series APF compensators. Standard split DC-link capacitors with a 4700 μF capacity are used at the shunt APF and each one stores the reactive power from the unbalanced non-linear demand. After that, a 3 mH L-typed filter is connected to the shunt compensator output, and switching ripples are reduced by connecting a 3.6 mH L-typed filter to the series APF. The DC-link reference capacitor voltage in this investigation is 700 V. In order to validate the significance of UPQC after connecting the external support of DC-link, the performance of the proposed approach is analyzed in a comparative manner. Performance simulated by UPQC that connected with PV and BESS (with PV-BESS) as external support of DC-link capacitor is compared with standard conventional UPQC (without PV-BESS). Additionally, the PV-BESS-UPQC is evaluated using the suggested STF technique for the compensator controller and contrasted with the standard conventional SRF-PLL combined with a reference current generation using the moving average filter (MAF) filter technique (also referred to as the SRF-MAF technique) in terms of performance.

CONNECTING PV EXTERNAL SOURCE USING UPQC USE OF STF TECHNIQUE:

Scenario A: **Maintain Constant Irradiance at 45°C by Balancing Harmonic Source Voltage with Nonlinear Load at 800 w/m2.**

Fig. 5 shows the PV-BESS-UPQC performance in relation to source voltage harmonics at PCC and the harmonic and sag combination. In accordance with Malaysia tropical climate, the temperature is kept at 45 degrees Celsius and the radiation level is kept constant at 800 W/m2. Grid voltages, series compensated voltages, load voltages, load currents, shunt compensated currents, and source currents are the many signals that are seen. Fig.5(A) shows that there are voltage harmonics from 0.3 to 0.45 seconds, a combination of voltage harmonic and voltage sag of 0.7 pu from 0.6 to 0.65 seconds, and a combination of voltage harmonic and voltage sag of 0.4 pu from 0.65 to 0.7 seconds. In such cases, the series compensator injects a suitable voltage VSE to reduce the source voltage, VS, during the voltage sag condition, as shown in Fig. 5(B), and maintain the load voltage, VL, at the rated value. Figure 5(C) shows that the load voltage is sinusoidal and matches the rated voltage. The distorted load current, iL, produced by the unbalanced non-linear load is displayed in Fig. 5(D). In this study, the three-phase imbalance load is taken into account. Due to the use of the non-linear load, the shunt compensator maintains the sinusoidal grid current by mitigating the source current, iS, by injecting a current iSH, as seen in Fig. 5(E). In Fig. 5(F), the sinusoidal grid current is shown. Fig.6(A) shows

ISSN: 2278-4632
Vol-15, Issue-04, No.03, April: 2025

that the DC link voltage remains constant at 700 V during both the voltage harmonic and the voltage sag combination. Fig.6(B) shows the PV current of around 46.2 A, and Figure 6(C) shows the PV power of 32 KW. Figure 6(D) shows the DC link power, which is raised between 0.3 and 0.45 seconds to compensate for the voltage harmonics. Additionally, in order to reduce harmonics and maintain the load in the event that the source voltage is insufficient, the DC power is raised between 0.6 and 0.75 seconds. The BESS power is shown in Fig. 6(E), where it is evident that it increases slightly between 0.3 and 0.45 seconds and slightly more between 0.6 and 0.75 seconds when the harmonics and sag occur. This is because the BESS current increases during these times. Fig. 6(F) displays the state of charge (SOC), which allows the charging activity of the BESS to be observed during the procedure.

Fig. 7(A) displays the THD for current under voltage harmonic conditions. It is evident that the THD, at 2.05%, is quite low. Furthermore, the THD for current under voltage harmonic with sag condition is displayed in Fig. 7(B), where it is evident that the THD is just 2.09%. Additionally, the THD for voltage is displayed in Fig. 7(C), where it is just 0.28%. Each of these THD outcomes satisfies IEEE standard 519. It is evident from Fig. 8 that the capacitor voltage rises quite quickly. The capacitor voltage reached the target value at 0.01 seconds. Rapid compensation by the series compensator and the shunt compensator may be carried out after the capacitor voltage reaches the target voltage more quickly.

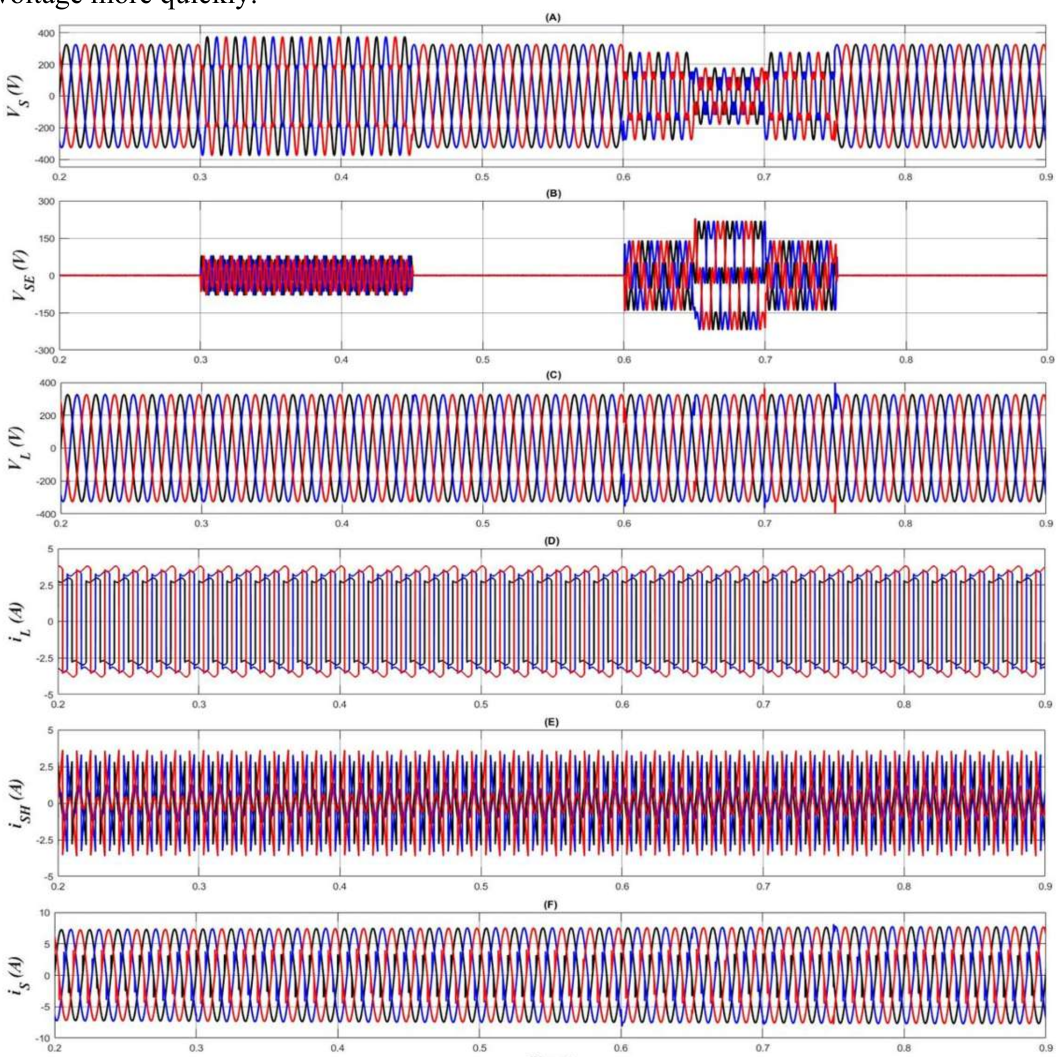

ISSN: 2278-4632
Vol-15, Issue-04, No.03, April: 2025

Fig. 5. Simulation waveform obtained under Case Study A for UPQC connected to PV-BESS, comprising (A) three-phase source voltage (B) series APF injection voltage (C) load voltage (D) load current (E) shunt APF injection current (F) source current.

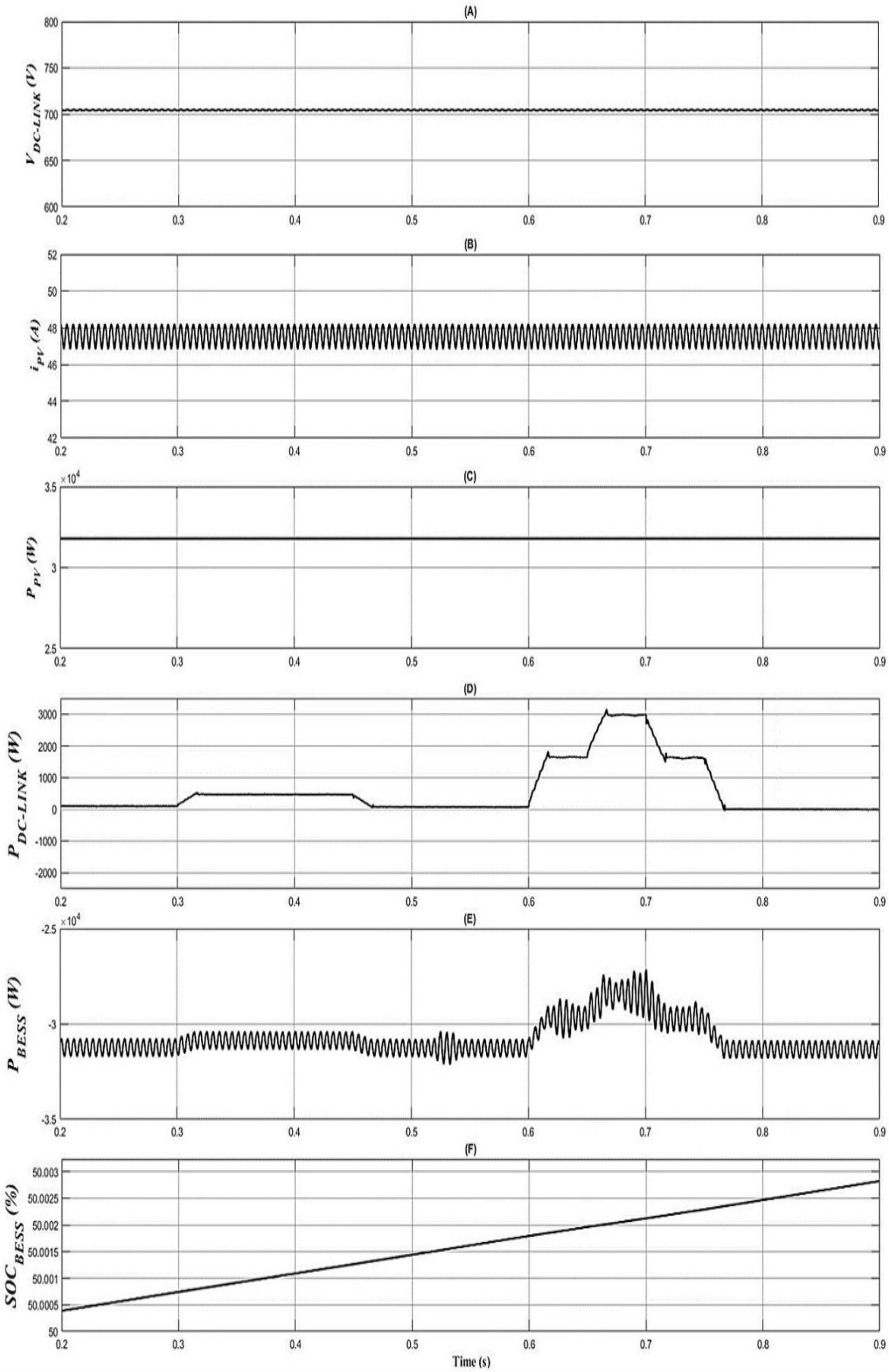

Fig.6. Simulation results obtained under Case Study 1 for UPQC connecting to PV-BESS, including (A) DC-Link Voltage (B) PV Current (C) PV Power (D) DC-Link Output Power (E) BESS Power (F) BESS SOC

CONCLUSION:

Three-phase UPQC architecture is being studied in light of complicated power quality issues, which include a combination of voltage sags, swells and harmonics as well as voltage interruption in the event of an imbalanced and distorted voltage grid. The network gains active power capacity when the BESS and PV are integrated with the UPQC. The primary advantage of BESS integration with UPQC is that it enables the system to both provide and absorb PV active power. The shortage of renewable energy supplies can be addressed by implementing a BESS as renewable energy is not entirely dependable due to its environment-dependent feature. Ultimately, it can be concluded that the BESS and PV connected to UPQC may be a suitable substitute in distributed generation to improve the modern distribution system power quality. Because of the PV-BESS system's constant supply, the DC link voltage remains steady. As a result, it can simplify the algorithm for DC-link voltage control. The shunt and series APF compensator effectively use the STF-UVG technology for synchronization phases to provide reference voltage and current. Therefore, in order to guarantee system stability and attain almost unity power factor, the UPQC is designed independently of the PLL components and current and voltage mitigation is accomplished effectively in accordance with the grid state. The proposed technique use verified that the grid current harmonics adhere to IEEE-519. Lastly, it is important to note that the proposed approach offers the potential to improve the grid power system overall efficiency.

REFERENCES:

[1] IEEE Standards Coordinating Committee 22 on Power Quality, IEEE Recommended Practice for Monitoring Electric Power Quality, vol. 2009, no. June. 1995.

[2] D. De Yong, S. Bhowmik, and F. Magnago, "Optimized Complex Power Quality Classifier Using One vs. Rest Support Vector Machines," Energy Power Eng., vol. 09, no. 10, pp. 568–587, 2017.

[3] A. Javadi, A. Hamadi, L. Woodward, and K. Al-Haddad, "Experimental Investigation on a Hybrid Series Active Power Compensator to Improve Power Quality of Typical Households," IEEE Trans. Ind. Electron., vol. 63, no. 8, pp. 4849–4859, 2016.

[4] A. Javadi, L. Woodward, and K. Al-Haddad, "Real-Time Implementation of a Three-Phase THSeAF Based on a VSC and a P+R Controller to Improve the Power Quality of Weak Distribution Systems," IEEE Trans. Power Electron., vol. 33, no. 3, pp. 2073–2082, 2018.

[5] M. A. Mansor, M. M. Othman, I. Musirin, and S. Z. M. Noor, "Dynamic voltage restorer (DVR) in a complex voltage disturbance compensation," Int. J. Power Electron. Drive Syst., vol. 10, no. 4, pp. 2222–2230, 2019.

[6] A. Ghosh and G. Ledwich, "Compensation of distribution system voltage using DVR," IEEE Trans. Power Deliv., vol. 17, no. 4, pp. 1030–1036, 2002.

[7] S. Jothi Basu and M. K. Mishra, "A control scheme for storageless DVR based on characterization of voltage sags," IEEE Trans. Power Deliv., vol. 29, no. 5, pp. 2261–2269, 2014.

[8] A. Farooqi, M. M. Othman, A. F. Abidin, S. I. Sulaiman, and M. A. M. Radzi, "Mitigation of power quality problems using series active filter in a microgrid system," Int. J. Power Electron. Drive Syst., vol. 10, no. 4, pp. 2245–2253, 2019.

[9] C. Kumar and M. K. Mishra, "Operation and Control of an Improved Performance Interactive DSTATCOM," IEEE Trans. Ind. Electron., vol. 62, no. 10, pp. 6024–6034, 2015.

[10] Y. Hoon, M. A. M. Radzi, M. K. Hassan, and N. F. Mailah, "Control algorithms of shunt active power filter for harmonics mitigation: A review," Energies, vol. 10, no. 12, 2017.

[11] L. B. Garcia Campanhol, S. A. Oliveira da Silva, and A. Goedtel, “Application of shunt active power filter for harmonic reduction and reactive power compensation in threephase four-wire systems,” IET Power Electron., vol. 7, no. 11, pp. 2825–2836, 2014.

[12] Y. Hoon, M. A. M. Radzi, M. K. Hassan, and N. F. Mailah, “Operation of Three-Level Inverter-Based Shunt Active Power Filter under Nonideal Grid Voltage Conditions with Dual Fundamental Component Extraction,” IEEE Trans. Power Electron., vol. 33, no. 9, pp. 7558–7570, 2018.

[13] E. Hossain, M. R. Tur, S. Padmanaban, S. Ay, and I. Khan, “Analysis and Mitigation of Power Quality Issues in Distributed Generation Systems Using Custom Power Devices,” IEEE Access, vol. 6, no. c, pp. 16816–16833, 2018.

[14] H. Fujita and H. Akagi, “The unified power quality conditioner: The integration of series- and shunt-active filters,” IEEE Trans. Power Electron., vol. 13, no. 2, pp. 315–322, 1998.

[15] S. K. Khadem, M. Basu, and M. F. Conlon, “Intelligent islanding and seamless reconnection technique for microgrid with UPQC,” IEEE J. Emerg. Sel. Top. Power Electron., vol. 3, no. 2, pp. 483–492, 2015.

[16] J. M. Guerrero, P. C. Loh, T. L. Lee, and M. Chandorkar, “Advanced control architectures for intelligent microgridsPart II: Power quality, energy storage, and AC/DC microgrids,” IEEE Trans. Ind. Electron., vol. 60, no. 4, pp. 1263–1270, 2013.

[17] B. Han, B. Bae, H. Kim, and S. Baek, “Combined operation of unified power-quality conditioner with distributed generation,” IEEE Trans. Power Deliv., vol. 21, no. 1, pp. 330–338, 2006.

[18] K. Hasan, M. M. Othman, N. F. A. Rahman, M. A. Hannan, and I. Musirin, “Significant implication of unified power quality conditioner in power quality problems mitigation,” Int. J. Power Electron. Drive Syst., vol. 10, no. 4, p. 2231, 2019.

[19] C. K. Sundarabalan, Y. Puttagunta, and V. Vignesh, “Fuel cell integrated unified power quality conditioner for voltage and current reparation in four-wire distribution grid,” IET Smart Grid, vol. 2, no. 1, pp. 60–68, 2019.

[20] S. Devassy and B. Singh, “Design and Performance Analysis of Three-Phase Solar PV Integrated UPQC,” IEEE Trans. Ind. Appl., vol. 54, no. 1, pp. 73–81, 2018.

[21] L. B. G. Campanhol, S. A. O. Da Silva, A. A. De Oliveira, and V. D. Bacon, “Power flow and stability analyses of a multifunctional distributed generation system integrating a photovoltaic system with unified power quality conditioner,” IEEE Trans. Power Electron., vol. 34, no. 7, pp. 6241–6256, 2019.

